Effect of spectral band numbers on the retrieval of water column and bottom properties from ocean color data

Zhongping Lee and Kendall L. Carder

Using an optimization technique, we derived subsurface properties of coastal and oceanic waters from measured remote-sensing reflectance spectra. These data included both optically deep and shallow environments. The measured reflectance covered a spectral range from 400 to 800 nm. The inversions used data from each 5-, 10-, and 20-nm contiguous bands, including Sea-viewing Wide Field-of-view Sensor (SeaWiFS), moderate-resolution imaging spectrometer (MODIS), and a self-defined medium-resolution imaging spectrometer (MERIS) channels, respectively. This study is designed to evaluate the influence of spectral resolution and channel placement on the accuracy of remote-sensing retrievals and to provide guidance for future sensor design. From the results of this study, we found the following: (1) use of 10-nm-wide contiguous channels provides almost identical results as found for 5-nm contiguous channels; (2) use of 20-nm contiguous channels and MERIS provides comparable results with those with 5-nm contiguous channels for deep waters, but use of contiguous 20-nm channels perform better than MERIS for optically shallow waters; and (3) SeaWiFS or MODIS channels work fine for deep, clearer waters (total absorption coefficient at 440 nm $< 0.3\ m^{-1}$), but introduce more errors in bathymetry retrievals for optically shallow waters. The inclusion of the 645-nm MODIS land band in its channel set improves inversion returns for both deep and shallow waters.

OCIS codes: 200.4560, 010.4450, 290.1350, 120.0280, 120.4820.

1. Introduction

Since the successful demonstration of the Coastal Zone Color Scanner for remote measurement of pigment concentrations of oceanic waters, many ocean color sensors exist or are planned for launch by different countries and agencies.[1] Currently there are, for example, Sea-viewing Wide Field-of-view Sensor (SeaWiFS), moderate-resolution imaging spectrometer (MODIS), and Modular Optoelectric Scanner sensors available.[1] In 2001, there will be more sensors with increased wavelength combinations, such as MODIS-FM1 of the U.S., medium-resolution imaging spectrometer (MERIS) of Europe, and the Global Imager of Japan.[2] A few hyperspectral sensors are also being considered, such as the Coastal Ocean Imaging Spectrometer of the U.S.[2] With the increase in band number and resolution, a wider variety of spectral information can be obtained, which could lead to improved retrieval and a wider variety of environmental properties. Also, use of more channels for retrievals, no matter whether we use empirical or analytical methods, reduces the dependence on accuracy of a single channel. On the other hand, an increase in band numbers requires larger data storage devices and inevitably will also lead to a longer processing time for the collected data with increased expense. Also, partitioning the spectral domain too thinly will lead to reduced signal-to-noise ratios within a given channel. If the main objective for coastal and oceanic observations is to estimate pigment concentration, gelbstoff (colored dissolved organic matter), sediment loading, bottom depth, and bottom type, an ideal sensor does not necessarily need hyperspectral bands. It might be more suitable and cost-effective to have adequate band numbers with high spatial resolution and high signal-to-noise ratios.

The Coastal Zone Color Scanner has four channels in the visible domain for pigment retrieval of oceanic

At the time of this research, Z. Lee (zplee@monty.marine.usf.edu) and K. L. Carder were with the Department of Marine Science, University of South Florida, 140 Seventh Avenue, South, St. Petersburg, Florida 33701. Z. Lee is now with the Naval Research Laboratory, Code 7340, Stennis Space Center, Mississippi 39529.

Received 9 May 2001; revised manuscript received 29 October 2001.

0003-6935/02/122191-11$15.00/0

Table 1. Data Information

Area	Time	Chlorophyll-a Range (mg m^{-1})	Depth range
Monterey Bay	September, October 1989	1.3–3.7	Deep
North Atlantic	August 1991	1.3–3.6	Deep
Gulf of Mexico	October 1992, April, June 1993	0.05–50.6	Deep
Arabian Sea	November–December 1994	0.4–0.9	Deep
Bering Sea	April 1996	0.5–7.4	Deep
Key West, Fla.	July 1994, June 1997	0.1–1.5	3–11 m
Bahamas	May 1998	0.06–0.14	8–23 m
Florida Bay	May 1997	0.6–2.3	1–2 m
West Florida Shelf	April 1990	0.6–1.1	14–25 m
Tampa Bay (Fla.)	October 1998	2.6–8.5	8–18 m

waters. Because it lacks shorter wavelengths in the blue, it could not adequately separate or retrieve gelbstoff. It worked only for Case 1 waters.[3] One of the added channels on SeaWiFS and MODIS is at 412 nm, which provides a better tool for gelbstoff and pigment separation.[4,5] It is generally assumed that these two sensors, however, cannot perform well when the bottom is optically shallow.[2]

There are a few studies[6] with regard to the number of spectral channels required for coastal and oceanic remote sensing. Through factor analysis, Sathyendranath *et al.*[6] found that for offshore waters the number of wavelength bands can be reduced from 32 to 6 without loss of much spectral information. How that conclusion would change if their data included near shore and/or optically shallow waters and use of a nonlinear inversion process instead of linear ones,[1,6] however, was not discussed.

For this study we used measured hyperspectral data from both optically deep and shallow environments and inverted the remote-sensing reflectance spectra to derive the absorption coefficients for pigments and gelbstoff, the particle backscattering coefficients, bottom depths, and bottom albedos by an optimization technique.[7] The derived absorption values can easily be converted to concentrations of pigment or gelbstoff if their specific absorption coefficients are known. For the inversion process, we applied different wavelength combinations to evaluate their influence on retrieval results. These combinations include contiguous bands every 5 nm from 400 to 800 nm, or every 10 nm, or every 20 nm. They also include SeaWiFS and MODIS band combinations, and self-defined MERIS channels. Inversion results here show that a total number of channels of around 15 from 400 to 800 nm are adequate for remote-sensing applications in most coastal and oceanic waters.

2. Data

Data used in this study came from a variety of oceanic and coastal environments with a wide range of water types, covering waters such as the West Florida Shelf, the Gulf of Mexico, the Bering Sea, the Arabian Sea, near the Bahamas, and near Key West, Florida. Table 1 summarizes the data sources and their chlorophyll concentration ranges. Locations for these data can be found in Lee *et al.*[7,8] For each station, remote-sensing reflectance (R_{rs}), which is the ratio of the water-leaving radiance to downwelling irradiance just above the surface, was measured when the water was viewed at 30° from nadir and 90° from the solar plane by use of a handheld spectroradiometer. The spectroradiometer covered the spectral range from ~360 to 900 nm, with a channel spacing of ~2 nm and a spectral resolution of 2.5 nm. The data processing method is as presented in the SeaWiFS protocols.[9]

Figure 1 shows examples of some measured R_{rs} spectra. For all the data (164 stations), chlorophyll concentration ranged from 0.05 to 50.0 mg/m^3. For the optically shallow waters (40 stations), the water depths ranged from 0.8 to 25.0 m. Note that reflectance peak wavelengths vary widely in the 400–600-nm range for different environmental properties.

3. Remote-Sensing Reflectance Model

In the past three decades, extensive studies were carried out to relate explicitly reflectance with in-water constituents.[3,7,10–15] For the satellite remote-sensing domain[14] and ignoring contributions from inelastic scattering,[16,17] we can express R_{rs} as[7]

$$R_{rs} \approx \frac{0.52\, r_{rs}}{1 - 1.56\, r_{rs}}, \tag{1}$$

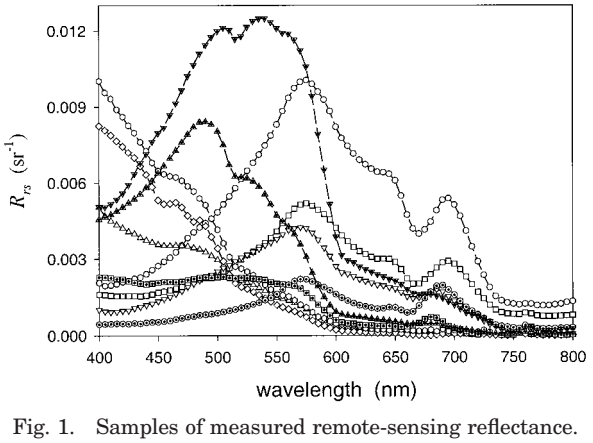

Fig. 1. Samples of measured remote-sensing reflectance.

where r_{rs} (the subsurface remote-sensing reflectance or ratio of the upwelling radiance to downwelling irradiance evaluated just below the surface) is

$$r_{rs} \approx r_{rs}^{C} + r_{rs}^{B} \approx r_{rs}^{dp}\left(1 - \exp\left\{-\left[\frac{1}{\cos(\theta_w)} + \frac{D_u^{C}}{\cos(\theta_v)}\right]\kappa H\right\}\right) + \frac{1}{\pi}\rho \exp\left\{-\left[\frac{1}{\cos(\theta_w)} + \frac{D_u^{B}}{\cos(\theta_v)}\right]\kappa H\right\}. \quad (2)$$

In approximation (2), r_{rs}^{C} and r_{rs}^{B} represent the water column and the bottom contributions, respectively; r_{rs}^{dp} represents the remote-sensing reflectance of optically deep waters; θ_w is the subsurface solar zenith angle, θ_v is the subsurface sensor viewing angle from nadir; ρ is the bottom albedo; κ is the attenuation coefficient and is defined as the sum of absorption and backscattering coefficients; D_u^{C} and D_u^{B} are the path-elongation factors for photons scattered by the water column and photons scattered by the bottom, respectively; and H is the bottom depth. There is

$$\kappa \equiv a + b_b, \quad (3)$$

with a as the total absorption coefficient, b_b as the total backscattering coefficient, and

$$b_b(\lambda) = b_{bw}(\lambda) + b_{bp}(\lambda), \quad (4)$$

where b_{bw} is the backscattering coefficient for pure seawater with values taken from Morel,[18] and b_{bp} is the backscattering coefficient of suspended particulates. The term r_{rs}^{dp} is further expressed as[19]

$$r_{rs}^{dp} \approx g_w \frac{b_{bw}}{a + b_b} + g_p \frac{b_{bp}}{a + b_b}, \quad (5)$$

where g_w is an empirical parameter that approximates 0.115 (Ref. 19) for the satellite remote-sensing domain[14] and g_p is a parameter that describes the contribution from suspended particulates. For sensor viewing at 30° from nadir and 90° from the solar plane g_p can be well described by the formula[19]

$$g_p \approx 0.184[1 - 0.602 \exp(-3.852u_p)], \quad (6)$$

where

$$u_p \equiv \frac{b_{bp}}{a + b_b}. \quad (7)$$

The optical path-elongation factors for scattered photons from the water column (D_u^{C}) and the bottom (D_u^{B}) are[7]

$$D_u^{C} \approx 1.03(1 + 2.4u)^{0.5}, \quad D_u^{B} \approx 1.04(1 + 5.4u)^{0.5}, \quad (8)$$

where

$$u \equiv \frac{b_b}{a + b_b}. \quad (9)$$

Note that it is the combination of approximations (1), (2), (5), (6), and (8) and Eqs. (3), (4), (7), and (9) that provides the expression for R_{rs}. For brevity, wavelength dependence is not explicitly included unless required for clarity.

4. Inversion Method

The model-inversion method is the same optimization approach as that used by Lee *et al.*[7,20] Briefly, to derive in-water properties analytically, total absorption $a(\lambda)$ is separated explicitly as[21,22]

$$a(\lambda) = a_w(\lambda) + a_\phi(\lambda) + a_g(\lambda). \quad (10)$$

Values of $a_w(\lambda)$, the absorption coefficients of pure water, were taken from Pope and Fry.[23] $a_\phi(\lambda)$, the absorption coefficient of phytoplankton pigments, is simulated as[7]

$$a_\phi(\lambda) = [a_0(\lambda) + a_1(\lambda) \ln(P)]P, \quad (11)$$

where $P = a_\phi(440)$, the phytoplankton absorption coefficient at 440 nm. The empirical coefficients for $a_0(\lambda)$ and $a_1(\lambda)$ are presented by Lee *et al.*[7,20] $a_g(\lambda)$, the absorption coefficient of gelbstoff and detritus, is expressed as[22,24,25]

$$a_g(\lambda) = G \exp[-S(\lambda - 440)], \quad (12)$$

where $G = a_g(440)$; S is the spectral slope that has been reported for the 0.011–0.021-nm^{-1} range for the waters studied[25,26]; and $a_g(\lambda)$ here is the sum of gelbstoff and detritus absorption spectra, so we used an S value of 0.015 nm^{-1} as the representative average between that for detritus and that for gelbstoff in our inversion process. $b_{bp}(\lambda)$ in Eq. (4) is written as

$$b_{bp}(\lambda) = Б\left(\frac{640}{\lambda}\right)^{Y}, \quad (13)$$

where $Б = b_{bp}(640)$ is the effective particle backscattering coefficient at 640 nm since dependencies on solar zenith angle and particle phase function are included.[19] The spectral dependence parameter Y is estimated by the empirical relationship[27]

$$Y \approx 3.44[1 - 3.17 \exp(-2.01\chi)], \quad (14)$$

where $\chi = R_{rs}(440)/R_{rs}(490)$. We keep Y within the range from 0 to 2.5.

A 550-nm normalized, sand-albedo shape [$\rho_{sd}^{+}(\lambda)$, Ref. 7] was used to model $\rho(\lambda)$. Note that only sandy or deep environments were covered in this data set. Therefore $\rho(\lambda)$ is expressed as

$$\rho(\lambda) = B\ \rho_{sd}^{+}(\lambda), \quad (15)$$

where B is the bottom albedo value at 550 nm.

With the above considerations, approximation (1) is described by use of five environmental parameters: P, G, Б, B, and H, which are often desired for environmental observations and coastal management decisions. A computer program has been developed to invert the values of the five parameters from measured R_{rs} by optimization. This optimization is ef-

fectively a predictor–corrector, model-inversion scheme, achieved by adjustment of the values of P, G, Б, B, and H to minimize a predefined error function, which is[27]

$$\text{error} = \frac{\left[\sum_{400}^{670}(R_{rs}-\hat{R}_{rs})^2 + \sum_{750}^{800}(R_{rs}-\hat{R}_{rs})^2\right]^{0.5}}{\sum_{400}^{670}R_{rs} + \sum_{750}^{800}R_{rs}}, \quad (16)$$

where $\hat{R}_{rs}$ represents values from approximation (1) and R_{rs} represents values from the measurements. The cutoff between 670 and 750 nm is required because no term is included in the model to express the solar-stimulated chlorophyll fluorescence presented in the measured data. Also, this spectral range is greatly affected by the absorption of water vapor that is quite variable. The computer program automatically changes the values of P, G, Б, B, and H until the error reaches a minimum. At that point, values for P, G, Б, B, and H are then considered to be derived.

Using data every 5 nm (65 effective channels from 400 to 800 nm as wavelengths from 670 to 750 nm were excluded), Lee *et al.*[7] demonstrated that those properties could be adequately retrieved from remote-sensing reflectance by use of the optimization approach. What is not yet known from use of the same optimization approach is how spectral channel number and position would influence the retrievals, since many current sensors have only a few preselected wavelength bands.

To observe the effects of a reduced number of channels on retrievals by use of this optimization approach, we carried out inversions for data of every 5-nm contiguous bands (E5), every 10 nm (E10), and every 20 nm (E20) in addition to the MERIS, MODIS, and SeaWiFS wavelength combinations. The 12-band MERIS simulation here is what we define as optimum MERIS channels, which can be programmed after launch.[1] This definition does not necessarily match the actual MERIS band configuration that may be programmed for use at any given time. We also added the 645-nm land band to the MODIS ocean bands (8–15) to assemble a MODIS2 configuration to indicate a possible improvement for coastal waters, although its bandwidth (50 nm) was not considered. Table 2 summarizes the wavelength combinations in this study. Note that all the calculations were made without consideration of actual signal-to-noise ratios for existing sensors, when we considered only the band number and placement in the analyses.

Bands at longer wavelengths, e.g., 750 and 780 nm for MERIS, normally reserved for atmospheric correction, were retained in this study because the remote-sensing reflectance at those bands was not zero for turbid coastal waters. For practical satellite image processing, R_{rs} values for these wavelengths could be estimated by the methods of Bricaud and Morel[28] or that of Arnone *et al.*[29]

Also, for SeaWiFS and MODIS sensors, the 670- or 667-nm bands, respectively, were not used for high-chlorophyll waters, as the R_{rs} values at those bands are often contaminated by the chlorophyll-a fluorescence (see, e.g., Carder and Steward[11]). Although the 670-nm band was included for E5 or E10 combinations, the R_{rs} value at that wavelength has only a minimal effect on retrievals as it has very limited weight on the error function [Eq. (16)] when there are a large number of channels involved in the inversion.

Table 2. Wavelength Selections

Sensor	Wavelengths	Effective Number of Bands[a]
E5	400–800 nm, every 5 nm	65
E10	400–800 nm, every 10 nm	33
E20	400–800 nm, every 20 nm	17
MERIS	410, 440, 460, 490, 520, 550, 580, 600, 620, 650, 750, 780	12
MODIS	412, 443, 488, 531, 551, 667, (680), 748	7[b]
SeaWiFS	412, 443, 490, 510, 555, 670, 765	7
MODIS2	412, 443, 488, 531, 551, 645, 667, (680), 748	8[b]

[a]Wavelengths around 680 nm were not included in the inversion process; see text for details.
[b]The 680-nm band was not used in the inversion process because of chlorophyll-a fluorescence.

5. Results and Discussion

Ideally we should compare all inversion results to the true field values to evaluate the performance of each inversion. Unfortunately, not many stations have all the measurements needed (e.g., gelbstoff absorption, backscattering, bottom albedo, bottom depth), and, more importantly, each field-measured quantity contains its own measurement errors. It would be difficult to separate errors that are due to channel-number reduction from that due to measurement uncertainty. Lee *et al.*,[7] however, found that accuracy of the inversion process itself was within approximately 5% for depth and 3% for absorption for errors and noise-free data. Since our focus here is to analyze the inversion errors that are due to channel-number reduction, we used the inversion results from E5 as the standard for comparison with inversion results from all the other channel combinations.

The percentage difference for each property is calculated as[4]

$$\delta = \exp\left[\text{mean}\left|\ln\left(\frac{Q_i^{\text{inv}}}{Q_i^{\text{std}}}\right)\right|\right] - 1. \quad (17)$$

Here, Q_i is the ith quantity of Q [e.g., $a(440)$], Q^{inv} represents the inverted value, and Q^{std} represents the standard. Table 3 summarizes the percentage differences for the five major properties derived by use of each sensor in Table 2. Note that model, measurement, and algorithm uncertainties must be added to evaluate the total accuracies of a sensor by use of this spectral-inversion technique. Total accuracies of the high-spectral-resolution inversion ap-

Table 3. Percentage Differences When Compared with the Results from Each 5-nm Contiguous Band

Properties	E10	E20	MERIS	MODIS	SeaWiFS	MODIS2
$a(440)$	0.004	0.011	0.014	0.052	0.066	0.030
P	0.021	0.062	0.061	0.135	0.148	0.109
G	0.011	0.035	0.034	0.062	0.082	0.042
Б	0.005	0.016	0.028	0.103	0.104	0.059
H	0.013	0.014	0.055	0.137	0.190	0.095
B	0.025	0.026	0.095	0.165	0.218	0.146

proach have been discussed for ship-derived[7] and aircraft-derived data sets.[20]

A. Total Absorption Coefficient at 440 nm

The total absorption coefficient is a major component for determination of photon availability at depth,[30–32] and it is an important indicator of water clarity. We thus compared this quantity first. Figure 2 shows the comparison of retrieved $a(440)$ values. Figure 2(a) shows values for the entire data set, Fig. 2(b) shows those for optically shallow waters, and Fig. 2(c) shows expanded $a(440)$ values of less than 0.3 m^{-1}. For an $a(440)$ range of 0.02–2.0 m^{-1}, the percentage differences are less than 1% between E10 and E5, less than 1.1% between E20 and E5, approximately 1.4% between MERIS and E5, 5.2% between MODIS and E5, 6.6% between SeaWiFS and E5, and 3.0% between MODIS2 and E5 retrievals.

Larger percentage errors were observed with reductions of channel number and larger $a(440)$ values. The result in Fig. 2(c) indicates that the sensors in Table 2 perform well for the retrieval of $a(440)$ for clearer waters, even for waters with optically shallow bottoms [except for one SeaWiFS retrieval; see Fig. 2(b)]. This could be because (a) most shallow stations in this data set had adequate water-column contributions, and (b) most shallow stations were in clearer waters [$a(440) < 0.3$ m^{-1}; see Fig. 2(b)], providing a spectral transparency window in the blue-green range (490–530 nm). This range can be adequately covered by the SeaWiFS and MODIS channels (additional discussion about this follows)

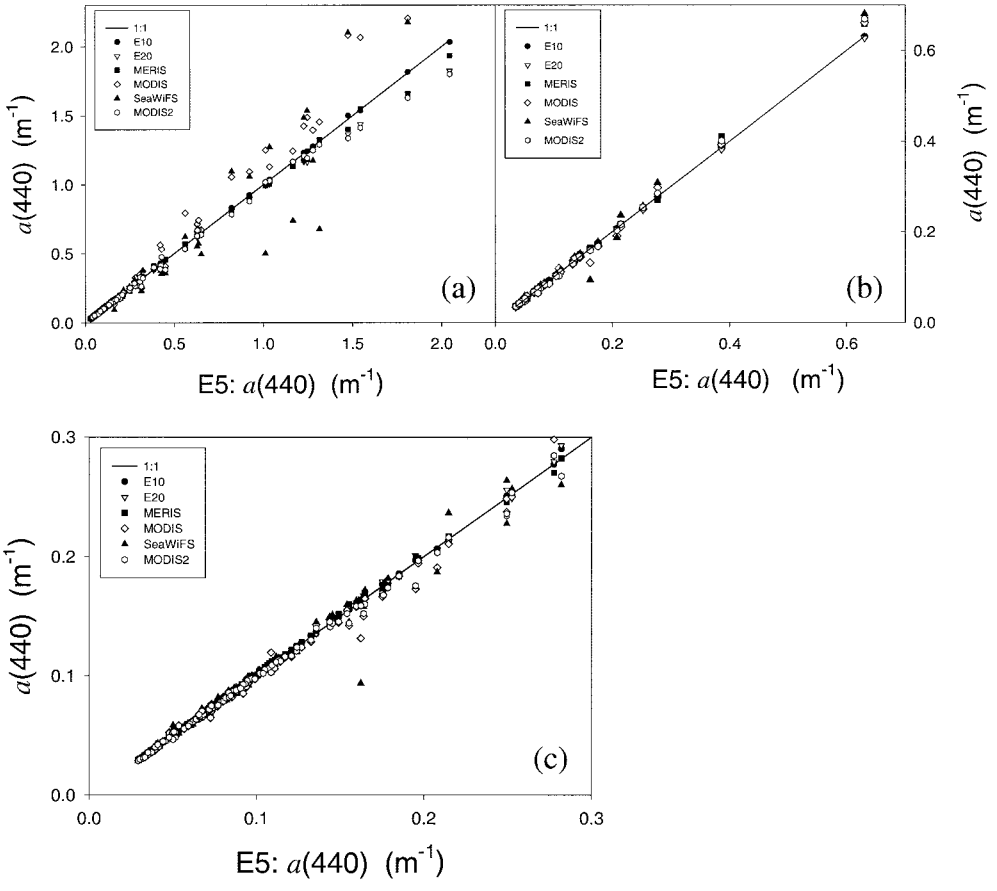

Fig. 2. Comparison of $a(440)$ retrievals for the sensors in Table 2: (a) for the entire data set, (b) for optically shallow waters only, (c) for $a(440) < 0.3$ m^{-1} only.

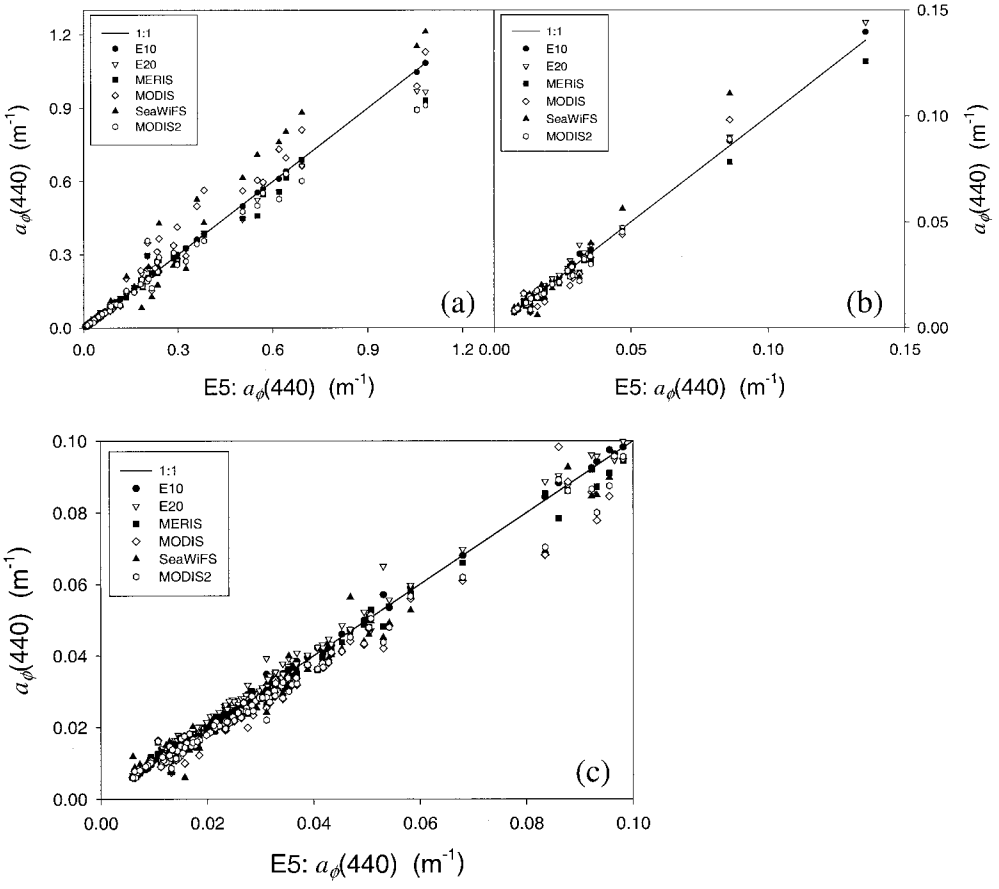

Fig. 3. Comparison of $a_\phi(440)$ retrievals for the sensors in Table 2: (a) for the entire data set, (b) for optically shallow waters only, (c) for $a_\phi(440) < 0.1$ m^{-1} only.

and separation of the water-column contribution from that of the bottom can be achieved. When $a(440)$ values increase as usually happens in turbid coastal waters, we found more errors and an increase in the number of spectral channels in the 560–660-nm range appears to be needed for better retrieval.

B. Pigment Absorption Coefficient

Figure 3 compares retrieved $a_\phi(440)$ values. Figure 3(c) highlights retrievals for values less than 0.1 m^{-1} (equivalent chlorophyll concentration is ~2 mg/m^3 according to the Morel model[32]). For an $a_\phi(440)$ range of 0.01–1.0 m^{-1}, the percentage differences are 2.1% between E10 and E5, 6.2% between E20 and E5, 6.1% between MERIS and E5, 13.5% between MODIS and E5, 14.8% between SeaWiFS and E5, and 10.9% between MODIS2 and E5 retrievals.

Larger differences were found for the retrieved pigment absorption coefficient than for the total absorption coefficient, because the waters in this study included many coastal stations, where the main absorbing component can be gelbstoff for blue-green wavelengths. The average $a_g(440)/a_\phi(440)$ ratio for this data set is 2.1, with an average ratio of 1.7 for deeper waters, and 3.5 for shallower waters. These ratios suggest that the absorption signals from pigments were strongly overshadowed by gelbstoff, making accurate pigment absorption retrieval more difficult, especially when there are a limited number of bands. For clearer waters, say $a_\phi(440) < 0.1$ m^{-1}, we saw much more consistent retrievals among the different channel selections [see Fig. 3(c)]. This suggests that for open ocean waters or clear shallow waters as in this data set, all the sensors including SeaWiFS and MODIS work fine for pigment retrievals. This result is also consistent with the findings of Sathyendranath *et al.*[6] and that of Mueller.[33] When the channel number is reduced from 32 to 6, only a small amount of spectral information is lost for offshore waters.

C. Gelbstoff Absorption Coefficient

Figure 4 compares retrieved $a_g(440)$ values, with the focus of Fig. 4(c) on retrievals for values less than 0.3 m^{-1}. Again, all the spectral combinations performed well for clearer waters, even for the optically shallow ones in this data set. Most of the variation appears for data with larger $a_g(440)$ values, where most data were from turbid coastal waters. Here the R_{rs} peak shifted from blue-green to green-orange wavelengths, but no channels in SeaWiFS and MODIS cover the 560–660-nm range. For the entire data set (0.01–1.2 m^{-1}), the differences are 1.1% be-

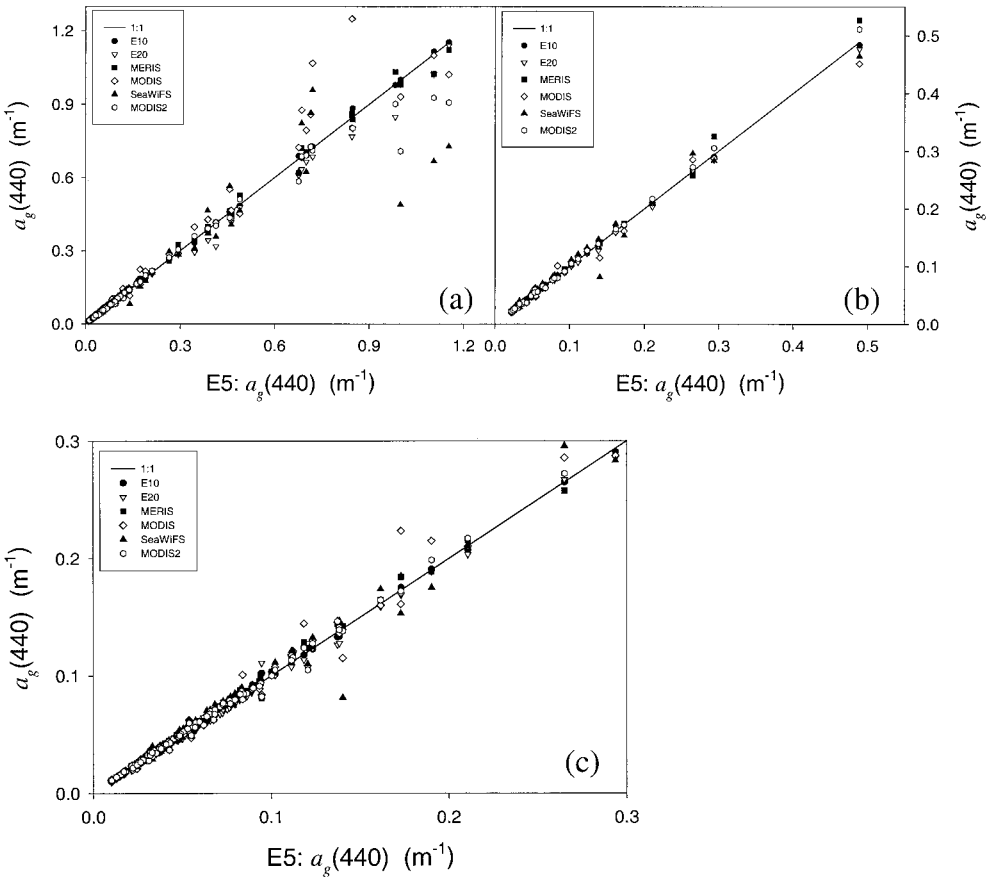

Fig. 4. Comparison of $a_g(440)$ retrievals for the sensors in Table 2: (a) for the entire data set, (b) for optically shallow waters only, (c) for $a_g(440) < 0.3$ m^{-1} only.

tween E10 and E5, 3.5% between E20 and E5, 3.4% between MERIS and E5, 6.2% between MODIS and E5, 8.2% between SeaWiFS and E5, and 4.2% between MODIS2 and E5 retrievals. The differences are larger than those found for the total absorption coefficient, but smaller than those for the pigment absorption coefficient. These larger differences are due to the additional error introduced in the process of decomposing the total absorption into separate components, and the fact that gelbstoff absorption played a larger role in the total absorption than did the pigment absorption at 440 nm for this data set.

D. Particle Scattering Coefficient

Figure 5 shows a comparison of retrievals of the effective particle backscattering values. The differences are 0.5% between E10 and E5, 1.6% between E20 and E5, 2.8% between MERIS and E5, 10.3% between MODIS and E5, 10.4% between SeaWiFS and E5, and 5.9% between MODIS2 and E5 retriev-

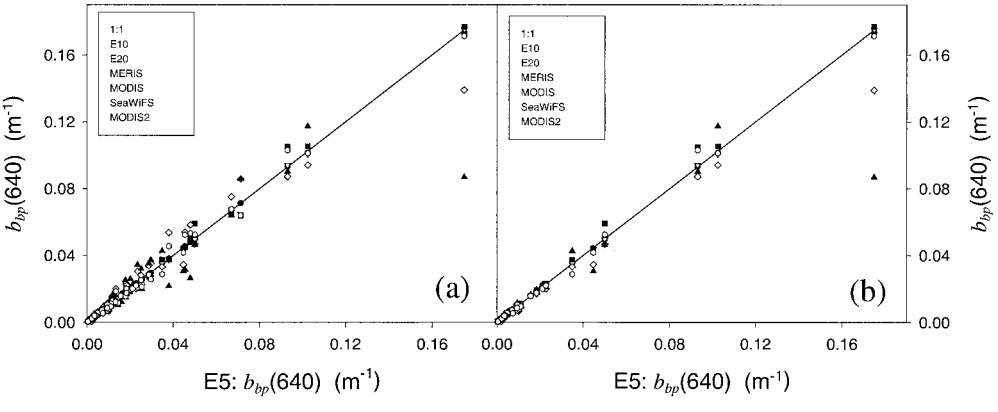

Fig. 5. Comparison of retrievals of the effective particle backscattering coefficient at 640 nm for the sensors in Table 2: (a) for the entire data set and (b) for optically shallow waters only.

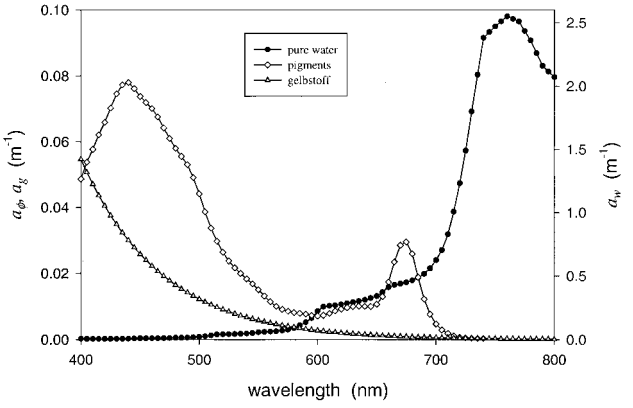

Fig. 6. Absorption curvatures of the three major components. Note the scale difference between the left and the right Y axes. a_ϕ and a_g spectra vary with concentrations, whereas the water spectrum is constant.

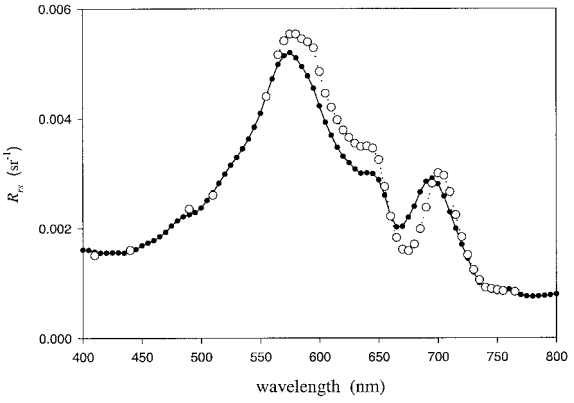

Fig. 7. Example of SeaWiFS retrieval in simulation of the entire R_{rs} spectrum: filled circles, the measured spectrum; open circle, a simulation by use of SeaWiFS retrievals. Apparently the simulation is a good match with the measured spectrum for SeaWiFS bands, but performs poorly for the extrapolated 570–650-nm range as there are no bands to force the simulation to match the measurement. The 670-nm band cannot be used because of the strong chlorophyll-a fluorescence expected there (not shown in simulation) for high-chlorophyll waters.

als. Most channel selections provide better retrievals for the particle backscattering coefficient than for pigment or gelbstoff absorption, although total absorption retrievals were more accurate. This is perhaps due to the fact that scattering is described by a function of one variable [Б in Eq. (13)], and this component dominates the scattering process at the red end of the spectrum. In contrast, absorption is described by a function of two variables (P and G), and the two compete with each other strongly in the inversion process.

When the water is optically shallow, however, we do see more errors introduced by separating photons from the bottom and those from the water column. The larger differences for MODIS and SeaWiFS retrievals of Б could be due to the fact that these two sensors have no spectral bands between 560 and 660 nm. They cannot accurately separate the signals from the water column and from the bottom for some optically shallow waters (more discussion about this follows).

For optically deep but turbid coastal waters, we also experienced difficulties in retrieving accurate scattering values using SeaWiFS or MODIS bands. This could be because R_{rs} values for deep waters are generally proportional to the ratio of b_b/a (Ref. 14), although in a nonlinear manner.[12,15] To estimate b_b from R_{rs} values, the value of a must be known or remain stable at least for one band, otherwise there will be no solution for b_b. This is because b_b affects R_{rs} with a similar weight across the entire spectrum, although b_b is generally somewhat larger at the shorter wavelength end. On the other hand, a affects R_{rs} in a spectrally selective manner (see, e.g., Fig. 6). Values of a vary significantly at the blue-green wavelengths as they depend heavily on the amount of pigment and gelbstoff present in the water. Values of a at the longer (red) wavelengths, however, are generally large and stable as they are dominated by the absorption values of water molecules. Therefore longer wavelengths play an important role in determination of the values of b_b (Ref. 34). Basically water absorption at longer wavelengths provides an internal scale or standard against which other properties are determined in the inversion process.

For the cases of SeaWiFS or MODIS with the 667 or 670 band affected by chlorophyll-a fluorescence, the useful longer wavelengths for high-chlorophyll cases are 555 and 765 nm (for SeaWiFS) or 551 and 748 nm (for MODIS). The absorption value at 765 nm (or 748 nm) is known as it is dominated by the values of pure water, but the R_{rs} values at those bands are more subject to errors in measurement that are due to low water-leaving radiances and atmospheric effects. At the same time, although R_{rs} values at 555 nm (or 551 nm) contain fewer measurement errors, the absorption values at those bands are quite variable for high-chlorophyll waters. A combination of these effects introduces more error in the retrieval of b_b and other properties for turbid coastal waters. Figure 7 shows an example of a good SeaWiFS retrieval that actually works poorly at the red end compared with the high-spectral-resolution R_{rs} curve.

Addition of a band at 645 nm (e.g., MODIS2), however, improves MODIS retrievals, since R_{rs} values at 645 nm are much larger than at 748 nm because of smaller absorption values (Fig. 6), and the total absorption is less variable than that at 555 nm. The addition of a channel somewhere between 610 and 625 nm[35] or the accurate removal of the chlorophyll fluorescence by use of existing 667/680 MODIS channels[36] would help even more when the water is turbid or the water has high-chlorophyll concentrations. This band addition (at 645 nm) or fluorescence correction (at 667/680 nm) has a limited effect for most open-ocean waters in which the signals from 620 to 680 nm are usually very small or close to zero and are difficult to measure with accuracy.

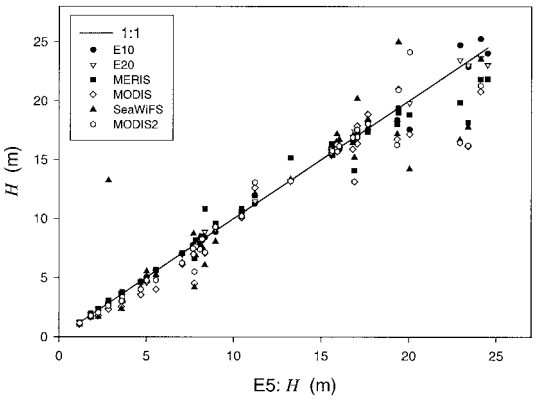

Fig. 8. Comparison of bathymetry retrievals for the sensors in Table 2.

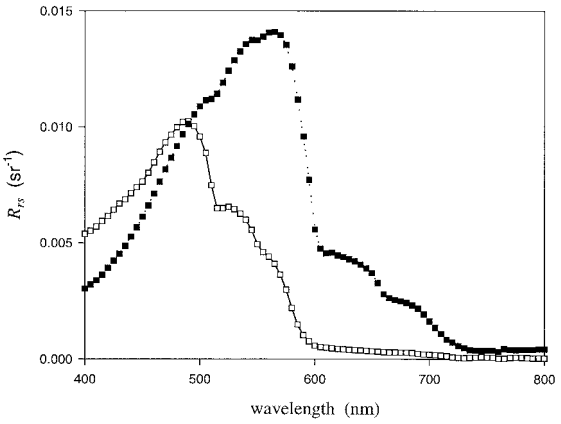

Fig. 9. Samples of remote-sensing reflectance for optically shallow waters.

E. Bottom Depth

Figure 8 compares bathymetry retrievals for optically shallow waters. The percentage differences are 1.3% between E10 and E5, 1.4% between E20 and E5, 5.5% between MERIS and E5, 13.7% between MODIS and E5, 19.0% between SeaWiFS and E5, and 9.5% between MODIS2 and E5 retrievals, respectively. As in the particle-scattering case, more error occurs for MODIS and SeaWiFS band selections because of the absence of spectral bands between 560 and 660 nm, where path and bottom-reflectance radiance can be best separated when the water becomes shallow.

Since strong bottom signals occur at wavelengths less than 600 nm but much less at longer wavelengths because of the two-way exponential attenuation [approximation (2)], a channel around 620 nm would detect mostly scattering effects with little bottom contribution. It would have no chlorophyll fluorescence contamination and would improve the separation of backscatter from the bottom reflectance. SeaWiFS and MODIS lack such channels, but the MODIS2 configuration does improve performance significantly as it has the 645-nm band.

Detection of the bottom strongly depends on the match of sensor channels to the water's spectral transparency window. The transparency window (e.g., note the peak values in Fig. 1) is a function of in-water properties. This window, which generally ranges from 470 to 570 nm, differs from place to place (see Fig. 9 for examples), and the limited number of bands preselected for SeaWiFS and MODIS cannot ensure detection of the strongest bottom signals from one area to another. Larger errors occur if the sensor channels do not match the peak of the transparency window of a given water body. For these reasons, some shallow-water cases were perceived as optically deep waters by SeaWiFS or MODIS sensors, and the retrieved bottom depth and bottom albedo were rendered unreliable.

F. Bottom Albedo

For optically shallow waters, the differences are 2.5% between E10 and E5, 2.6% between E20 and E5, 9.5% between MERIS and E5, 16.5% between MODIS and E5, 21.8% between SeaWiFS and E5, and 14.6% between MODIS2 and E5 retrievals. Again, larger errors occurred for MODIS and SeaWiFS band selections for the reasons discussed above.

We see slightly better retrievals for the five parameters when we use MODIS bands than when we use SeaWiFS bands based on this data set. A possible reason for this improvement could be due to the use of the 531-nm band for MODIS versus the 510-nm band for SeaWiFS, which leave a 45-nm gap in the SeaWiFS band coverage at green wavelengths but only a 30-nm gap for MODIS. Our data set contains many waters with high pigment and gelbstoff concentrations, with R_{rs} spectral peaks around 550 nm (see Fig. 1). Apparently the 490/531/551 combination (MODIS) provides a better measurement about this broad R_{rs} peak than the 490/510/555 combination (SeaWiFS) for turbid coastal waters. This band positioning effect, however, has little influence for clearer waters as their inversion is more dependent on the R_{rs} values in the blue to blue-green bands.

Effects of bandwidth[37] have not been included in this study. Preliminary analysis suggests that for an E10-like sensor there is little difference in the inversion results for deep waters by use of a 10-nm-wide bandwidth versus a 2-nm-wide bandwidth. SeaWiFS or MODIS has a limited number of bands, however, and we could expect the 20-nm-wide SeaWiFS bands to introduce slightly more error than would the 10-nm-wide MODIS bands.

6. Summary

Remote-sensing retrievals were carried out for different wavelength combinations, and all the inversion results were compared with the results obtained by use of 5-nm contiguous spectral bands. These retrievals suggest that sensors with 10-nm contiguous bands provide almost identical results as bands every 5 nm, whereas bands every 20 nm and the MERIS provide similar results as the 5-nm sensor for deep waters. For optically shallow waters, however, sensors with 20-nm contiguous bands provide better re-

sults than MERIS with regard to bottom depth and bottom albedo since they ensure better coverage of the transparency window of the water column.

SeaWiFS and MODIS channels work fine for clearer waters, but should be used with caution when applied to turbid coastal waters. SeaWiFS and MODIS channels introduce more errors in bathymetry retrievals for optically shallow waters, in general. They could, however, still provide reasonable retrievals with regard to the total absorption coefficient as long as there are adequate water-column contributions. Adding the 645-nm land band to the MODIS ocean-cover suite (MODIS2), however, improves all the retrievals.

These results indicate that the total number of channels around 15 that cover the 400–800-nm range are adequate for most coastal and oceanic remote-sensing applications. Atmospheric correction, which requires at least two bands in the infrared region,[38] was not considered here. Also, we must note that, although the data used in this study derive from a wide range of environments, they do not cover all possible coastal and oceanic environments, such as coral reefs, seagrass beds, and vertically structured coccolithophore and trichodesmium blooms, regions different and perhaps more challenging than those discussed here. For these kinds of environment, higher spectral resolution or some specially placed channels could help the retrievals. It is also necessary to point out that the conclusions are subject to the optimization method used and the limited objectives pursued here. If someone uses, for example, spectral derivatives,[39] certainly more spectral bands are required to work properly.

Financial support was provided by the following contracts and grants: NASA through NAS5-97137, NAS5-31716, and NAG5-3446; the Office of Naval Research through N00014-96-I-5013 and N00014-97-0006. Comments and suggestions by two anonymous reviewers are greatly appreciated. Z. P. Lee is also grateful for discussions at the Ocean Remote Sensing Institute of the Qingdao Ocean University supported by that Institute's visiting scholar fund.

References and Notes

1. A. Morel, "Minimum requirements for an operational ocean-colour sensor for the open ocean," IOCCG Rep. 1 (International Ocean-Colour Coordinating Group, Villefranche-sur-Mer, France, 1998).
2. S. Sathyendranath, "Remote Sensing of Ocean Colour in Coastal, and Other Optically-Complex, Waters," IOCCG Rep. 3 (International Ocean-Colour Coordinating Group, Dartmouth, Canada, 2000).
3. A. Morel and L. Prieur, "Analysis of variations in ocean color," Limnol. Oceanogr. **22,** 709–722 (1977).
4. K. L. Carder, S. K. Hawes, K. A. Baker, R. C. Smith, R. G. Steward, and B. G. Mitchell, "Reflectance model for quantifying chlorophyll *a* in the presence of productivity degradation products," J. Geophys. Res. **96,** 20599–20611 (1991).
5. K. L. Carder, R. F. Chen, Z. P. Lee, S. K. Hawes, and D. Kamykowski, "Semianalytic moderate resolution imaging spectrometer algorithms for chlorophyll *a* and absorption with bio-optical domains based on nitrate-depletion temperatures," J. Geophys. Res. **104,** 5403–5421 (1999).
6. S. Sathyendranath, F. E. Hoge, T. Platt, and R. N. Swift, "Detection of phytoplankton pigments from ocean color: improved algorithms," Appl. Opt. **33,** 1081–1089 (1994).
7. Z. P. Lee, K. L. Carder, C. D. Mobley, R. G. Steward, and J. S. Patch, "Hyperspectral remote sensing for shallow waters. 2. Deriving bottom depths and water properties by optimization," Appl. Opt. **38,** 3831–3843 (1999).
8. Z. P. Lee, K. L. Carder, R. G. Steward, T. G. Peacock, C. O. Davis, and J. S. Patch, "An empirical algorithm for light absorption by ocean water based on color," J. Geophys. Res. **103,** 27967–27978 (1997).
9. J. L. Mueller and R. W. Austin, *Ocean Optics Protocols for SeaWiFS Validation*, NASA Tech. Mem. 104566, Vol. 5, S. B. Hooker and E. R. Firestone, eds. (NASA Goddard Space Flight Center, Greenbelt, Md., 1992).
10. H. R. Gordon, O. B. Brown, and M. M. Jacobs, "Computed relationship between the inherent and apparent optical properties of a flat homogeneous ocean," Appl. Opt. **14,** 417–427 (1975).
11. K. L. Carder and R. G. Steward, "A remote-sensing reflectance model of a red tide dinoflagellate off West Florida," Limnol. Oceanogr. **30,** 286–298 (1985).
12. H. R. Gordon, O. B. Brown, R. H. Evans, J. W. Brown, R. C. Smith, K. S. Baker, and D. K. Clark, "A semianalytic radiance model of ocean color," J. Geophys. Res. **93,** 10909–10924 (1988).
13. J. T. O. Kirk, "Volume scattering function, average cosines, and the underwater light field," Limnol. Oceanogr. **36,** 455–467 (1991).
14. A. Morel and B. Gentili, "Diffuse reflectance of oceanic waters. II. Bidirectional aspects," Appl. Opt. **32,** 6864–6879 (1993).
15. Z. P. Lee, K. L. Carder, C. D. Mobley, R. G. Steward, and J. S. Patch, "Hyperspectral remote sensing for shallow waters. I. A semianalytical model," Appl. Opt. **37,** 6329–6338 (1998).
16. R. H. Stavn and A. D. Weidemann, "Optical modeling of clear ocean light fields: Raman scattering effects," Appl. Opt. **27,** 4002–4011 (1988).
17. Z. P. Lee, K. L. Carder, S. K. Hawes, R. G. Steward, T. G. Peacock, and C. O. Davis, "Model for interpretation of hyperspectral remote-sensing reflectance," Appl. Opt. **33,** 5721–5732 (1994).
18. A. Morel, "Optical properties of pure water and pure sea water," in *Optical Aspects of Oceanography*, N. G. Jerlov and E. S. Nielsen, eds. Academic, New York, 1974), pp. 1–24.
19. Z. P. Lee, K. L. Carder, and K. P. Du, "Particle phase function and remote-sensing reflectance model: a revisit," presented at the Ocean Color Research Team Meeting, San Diego, Calif., May 21–24, 2001.
20. Z. P. Lee, K. L. Carder, R. F. Chen, and T. G. Peacock, "Properties of the water column and bottom derived from Airborne Visible Infrared Imaging Spectrometer (AVIRIS) data," J. Geophys. Res. **106,** 11639–11651 (2001).
21. H. R. Gordon, R. C. Smith, and J. R. V. Zaneveld, "Introduction to ocean optics," in *Ocean Optics VI*, S. Q. Duntley, ed., Proc. SPIE **208,** 1–43 (1980).
22. K. L. Carder, S. K. Hawes, K. A. Baker, R. C. Smith, R. G. Steward, and B. G. Mitchell, "Reflectance model for quantifying chlorophyll *a* in the presence of productivity degradation products," J. Geophys. Res. **96,** 20599–20611 (1991).
23. R. Pope and E. Fry, "Absorption spectrum (380–700 nm) of pure water. II. Integrating cavity measurements," Appl. Opt. **36,** 8710–8723 (1997).
24. A. Bricaud, A. Morel, and L. Prieur, "Absorption by dissolved organic matter of the sea (yellow substance) in the UV and visible domains," Limnol. Oceanogr. **26,** 43–53 (1981).
25. C. S. Roesler, M. J. Perry, and K. L. Carder, "Modeling *in situ*

phytoplankton absorption from total absorption spectra in productive inland marine waters," Limnol. Oceanogr. **34,** 1510–1523 (1989).
26. K. L. Carder, R. G. Steward, G. R. Harvey, and P. B. Ortner, "Marine humic and fulvic acids: their effects on remote sensing of ocean chlorophyll," Limnol. Oceanogr. **34,** 68–81 (1989).
27. Z. P. Lee, K. L. Carder, R. G. Steward, T. G. Peacock, C. O. Davis, and J. L. Mueller, "Remote sensing reflectance and inherent optical properties of oceanic waters derived from above-water measurements," in *Ocean Optics XIII*, S. G. Ackleson, ed., Proc. SPIE **2963,** 160–166 (1996).
28. A. Bricaud and A. Morel, "Atmospheric corrections and interpretation of marine radiances in CZCS imagery: use of a reflectance model," Oceanol. Acta. **7,** 33–50 (1987).
29. R. A. Arnone, P. Maritinolich, R. W. Gould, R. Stumpf, and S. Ladner, "Coastal optical properties using SeaWiFS," in *Ocean Optics XIV*, Kailua-Kona, Hawaii, 10–13 November 1998.
30. S. Sathyendranath, T. Platt, C. M. Caverhill, R. E. Warnock, and M. R. Lewis, "Remote sensing of oceanic primary production: computations using a spectral model," Deep-Sea Res. **36,** 431–453 (1989).
31. Z. P. Lee, K. L. Carder, J. Marra, R. G. Steward, and M. J. Perry, "Estimating primary production at depth from remote sensing," Appl. Opt. **35,** 463–474 (1996).
32. A. Morel, "Optical modeling of the upper ocean in relation to its biogenous matter content (Case I waters)," J. Geophys. Res. **93,** 10749–10768 (1988).
33. J. L. Mueller, "Ocean color spectra measured off the Oregon coast: characteristic vectors," Appl. Opt. **15,** 394–402 (1976).
34. Z. P. Lee and K. L. Carder, "Multiband analytical algorithm for deriving absorption and backscattering coefficients from remote-sensing reflectance for optically deep waters," Appl. Opt. submitted for publication.
35. M. R. Wernand, S. J. Shimwell, and J. C. DeMunck, "A simple method of full spectrum reconstruction by a five-band approach for ocean color application," Int. J. Remote Sens. **18,** 1977–1986 (1997).
36. Z. P. Lee and K. L. Carder are preparing a manuscript to be called "Applying MODIS channels to high chlorophyll-concentration waters after correcting chlorophyll fluorescence."
37. M. H. Wang, B. A. Franz, R. A. Barnes, and C. R. McClain, "Effects of spectral bandpass on SeaWiFS-retrieved near-surface optical properties of the ocean," Appl. Opt. **40,** 343–348 (2001).
38. H. R. Gordon and M. Wang, "Retrieval of water-leaving radiance and aerosol optical thickness over oceans with SeaWiFS: a preliminary algorithm," Appl. Opt. **33,** 443–452 (1994).
39. D. F. Millie, O. M. Schofield, G. J. Kirkpatrick, G. Johnsen, P. A. Tester, and B. T. Vinyard, "Detection of harmful algal blooms using photopigments and absorption signatures: a case study of the Florida red tide dinoflagellate, Gymnodinium Breve," Limnol. Oceanogr. **42,** 1240–1251 (1997).